Physical properties of the dense Kondo compounds YbXCu$_4$ (X=Au, Ag, In, Cd, Tl, and Mg) probed by ^{63}Cu NMR

T. Koyama, M. Matsumoto, T. Tanaka, H. Ishida, T. Mito, and S. Wada
Department of Material Science, Graduate School of Science & Technology, and Department of Physics, Faculty of Science, Kobe University, Nada, Kobe 657-8501, Japan

J. L. Sarrao
Los Alamos National Laboratory, Mail Stop K 764, Los Alamos, New Mexico 87545
(Received 25 May 2001; revised manuscript received 18 January 2002; published 9 July 2002)

We have carried out a systematic ^{63}Cu nuclear magnetic resonance (NMR) study on a set of ytterbium-based Kondo compounds YbXCu$_4$ with X=Au, Ag, In, Cd, Tl, and Mg. Splitting of the central NMR line due to a second-order electric-quadrupole interaction is of the order of magnitude of axial Knight shift, and the extent of splitting is controlled by changing applied field H. From the splitting of the central line, we have succeeded to deduce the values of both isotropic Knight shift $K_{\rm iso}$ and axial Knight shift $K_{\rm ax}$, taking a value of electric-quadrupole frequency determined by pure quadrupole resonance of ^{63}Cu. $K_{\rm iso}$ versus magnetic susceptibility χ plots for each of the compounds with X=Au, Ag, and In are roughly on a straight line. For YbAgCu$_4$ (Kondo temperature $T_K \sim 100$ K), both $K_{\rm iso}$ and the unit-cell volume v_c reach a local minimum around 40 K. We have found a linear relation between $K_{\rm iso}$ and v_c below 100 K, similar to that observed in YbInCu$_4$, indicating that the nonmagnetic behavior at low temperatures can be ascribed mainly to the Kondo volume expansion. In contrast, $K_{\rm iso}$ versus χ plots for YbCdCu$_4$ ($T_K \sim 220$ K) and YbMgCu$_4$ ($T_K \sim 860$ K) exhibit somewhat complex behavior: hyperfine field $H_{\rm hf}$ markedly increases coincident with the saturated behavior of χ for X=Cd below $\simeq 140$ K, and with the decrease in χ for X=Mg below ~ 260 K. $H_{\rm hf}$ originates mainly from transferred hyperfine coupling between Cu nucleus and Yb $4f$ moment, and the large increase in $H_{\rm hf}$ is conjectured to result from a variation of crystal-electric-field interactions as the system transforms into a mixed-valence state. The variation with the species of X atoms of temperature-independent on-site contribution K_s to the Knight shift is found to correlate with that of the electronic specific heat coefficient γ (except for X=Cd), each of which gives a measure of the density of states of conduction sf resonance bands. Finally, using the values of K_s, γ, and T_K, we have proposed a phase diagram for YbXCu$_4$ series, which corresponds to Doniach's phase diagram.

DOI: 10.1103/PhysRevB.66.014420 PACS number(s): 71.28.+d, 71.27.+a

I. INTRODUCTION

Recently, intensive experimental and theoretical investigations have been concentrated on characteristic properties shown by rare-earth compounds such as valence fluctuations, heavy-Fermion behavior, and magnetic ordering, which are associated with the extent of mixing J_{sf} between f electrons and conduction electron density. A set of isostructural ytterbium-based compounds YbXCu$_4$ with X=Au, Cu, Ag, In, Cd, Tl, and Mg has been shown to have Kondo temperatures T_K that range from about 1 to nearly 10^3 K and displays a rich variety of physical properties.[1] The compounds crystallize in a cubic AuBe$_5$ ($C15b$ type) crystal structure illustrated in Fig. 1. Yb and X atoms sit on distinct face centered cubic (fcc) sublattices at (0,0,0) (4a site) and (1/4,1/4,1/4) ($4c$ site), and are surrounded by space-filling Cu tetrahedra centered at (3/4,3/4,3/4) ($16e$ site). Among the YbXCu$_4$ series, the compounds with X=Ag, Au, and In have been rather well studied. YbAuCu$_4$ is characterized by nearly localized Yb^{3+} moments and crystal-electric-field (CEF) effects.[1–5] The magnetic susceptibility χ has a Curie-Weiss (CW-) type behavior except at very low temperatures and exhibits antiferromagnetic ordering below 1 K. T_K is estimated as $\simeq 2$ K, and the rather large linear specific heat coefficient $\gamma \sim 0.15$ J/mol K^2 indicates a formation of sf resonance bands. In contrast, YbInCu$_4$ exhibits the most extreme limit of mixed-valence behavior of Yb^{3+} and Yb^{2+}; a first-order isostructural valence transition occurs at T_V=40–50 K with a unit-cell volume expansion of 0.5%.[1,6–14] Data of χ exhibit the CW-type behavior in the high-temperature (HT) phase, and a strongly enhanced Pauli paramagnetism in the low-temperature (LT) phase. T_K for the

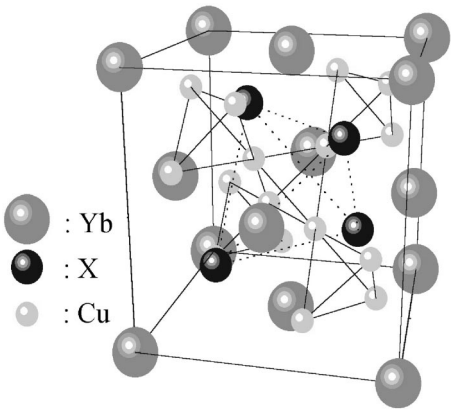

FIG. 1. Schematic crystal structure of YbXCu$_4$: C15b type. Closed circles: Yb, hatched circles: X, open circles: Cu.

TABLE I. Kondo temperatures, electronic specific heat coefficients, Weiss temperatures, and effective moments deduced from the magnetic susceptibility data above 100 K, transferred hyperfine fields for ^{63}Cu on the 16*e* site, on-site contributions to the Knight shift, and electric-quadrupole frequency for the YbXCu$_4$ series.

	T_K (K)	γ (J/mol K^2)	$\mu_{\rm eff}$ (μ_B)	θ_W (K)	$H_{\rm hf}$ (kOe/μ_B)	K_s (%)	ν_Q (4.2 K) (MHz)
YbAuCu$_4$	2 [a]	0.15 [c]	4.35	6	−0.63	0.33	8.96
YbAgCu$_4$	100 [b]	0.21 [c]	4.64	51	−0.72	0.46	10.66
YbCdCu$_4$	221 [a]	0.18 [c]	5.41	167	-0.52	0.15	11.36
YbMgCu$_4$	855 [a]	0.06 [c]		~72 [d]	+	~0.10	10.85
YbTlCu$_4$	740 [a]	0.03 [c]				0.20	13.2
YbInCu$_4$ (HT)	25 [e]		4.22	11	−0.45	0.17 [f]	14.92 (45 K)
YbInCu$_4$ (LT)	400 [e]	0.05				0.23 [f]	14.08

[a]Estimated in Ref. 1 from the zero-temperature magnetic susceptibility inferred from fitting the $\chi(T)$ data to the Bethe anzatz solution of the Coqblin Schrieffer model.
[b]Estimated from various experiments and theories.
[c]Referred from Refs. 10,14.
[d]Deduced from the $\chi(T)$ data above 300 K.
[e]Referred from Ref. 1.
[f]Referred from Ref. 29.

HT phase is estimated as ~25 K. YbAgCu$_4$ has been considered as being in a intermediate state between the localized and mixed-valence regimes.[2,3,15–21] It has a large γ of ~0.21 J/mol K^2, and T_K is estimated from various experiments and theories as ~100 K. The χ data have a local maximum around 40 K, that can be fit quantitatively to numerical predictions[22] of J=7/2 Coqblin-Schrieffer model[23] (a single impurity Anderson Hamiltonian in the Kondo limit). However, a number of investigations such as neutron scattering,[3] pure quadrupole resonance (PQR),[24] electron-spin resonance,[25] x-ray absorption, or photoelectron spectroscopy[20,26] have confirmed a strong J_{sf}, which is indicative of a mixed-valence system with nonmagnetic ground state. Compounds with X=Cd, Tl, and Mg have been relatively less studied;[1,27,28] each displays properties intermediate to those described above. The values of γ and T_K for the YbXCu$_4$ series reported previously are shown in Table I. Although the single-impurity Kondo model has qualitatively accounted for much of the physical properties,[1] universal behavior cannot be inferred by only accounting for variations in T_K.

In this paper, we report a systematic investigation of isotropic and axial Knight shifts and electric-quadrupole frequency of ^{63}Cu in the dense Kondo compounds YbXCu$_4$ with X=Au, Ag, Cd, Tl, and Mg, to deduce the varied impact of variations in effective valence and unit-cell volume, crystal-electric-field splitting and sf hybridization, that can define more clearly what we do not understand. The Knight shift is a measure of local magnetic susceptibility and provides information on the magnetic state of Yb ions through transferred hyperfine interactions. One can also estimate the density of states of conduction sf bands through the on-site contribution to the Knight shift. Value of the electric-quadrupole frequency provides information on the local electron distribution around Cu nuclei.

II. EXPERIMENTS

We used single-crystal specimens of YbXCu$_4$ with X=Au, Ag, Cd, Tl, and Mg. A superconducting-quantum-interference-device magnetometer was used to measure the magnetic susceptibility χ. Figure 2 shows the χ data plotted against temperature on a log-log scale for each of the compounds. χ for X=Ag, Tl, and Mg shows a local maximum around 40, 260, and 130 K, respectively, that has been known to be a characteristic of mixed-valence compounds. χ for X=Au shows a large CW-type increase down to 2 K,

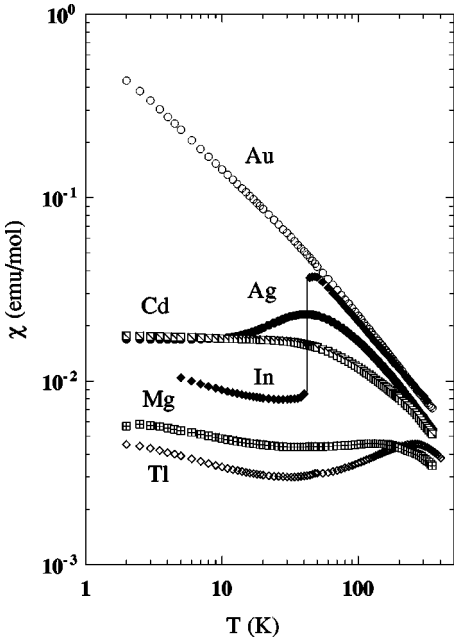

FIG. 2. Susceptibility as a function of temperature for YbXCu$_4$ with X=Au, Ag, In, Cd, Tl, and Mg.

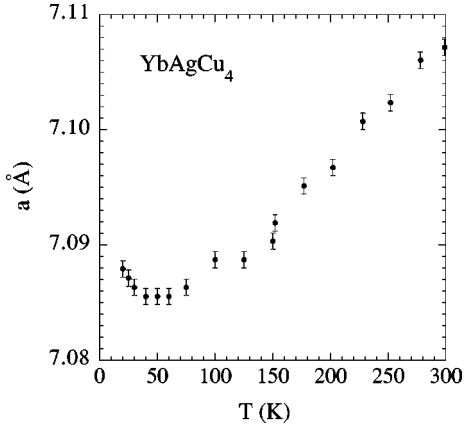

FIG. 3. Dependence of lattice constant a of $YbAgCu_4$ on the temperature, measured by low-temperature x-ray diffraction.

while that for $X=$Cd tends to saturate below about 50 K. From the CW-type behavior at high temperatures, we can estimate values of Weiss temperature θ_W, and effective magnetic moment $\mu_{\rm eff}$ for $X=$Au, Ag, and Cd. The results are summarized in Table I with the data for $X=$In referred from Ref. 29. It is worth noting that among the compounds $\mu_{\rm eff}$ for $X=$Cd is somewhat larger in magnitude than 4.54 μ_B for free Yb^{3+} ions.

For $YbAgCu_4$, we have observed a temperature dependence of the lattice constant a by x-ray diffraction measurements. As shown in Fig. 3, the value of a for $X=$Ag shows a broad minimum at around 40 K where the χ data exhibit the local maximum. For NMR and PQR measurements, we crushed the single crystal specimens into powder with grain size smaller than the skin depth. To obtain values of quadrupole frequency ν_Q, we have carried out PQR measurements of ^{63,65}Cu in zero field. The values of ν_Q for each of the compounds are summarized also in Table I, which are in good agreement with those reported previously for $X=$Au, Ag, and In,[24] and for $X=$Cd and Tl.[27,28]

The NMR experiments were carried out in a temperature range between 4.2 and about 250 K utilizing a wide-band phase-coherent spin-echo spectrometer. Figure 4 shows typical ^{63}Cu and ^{65}Cu NMR spectra observed for $YbMgCu_4$ at 4.2 K in a field sweeping procedure at a constant frequency

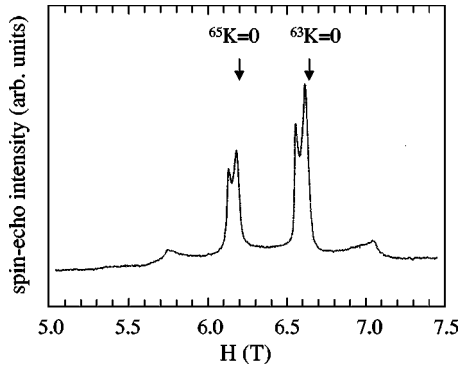

FIG. 4. ^{63}Cu and ^{65}Cu NMR spectra for $YbMgCu_4$ at 4.2 K measured at a constant frequency of 75 MHz.

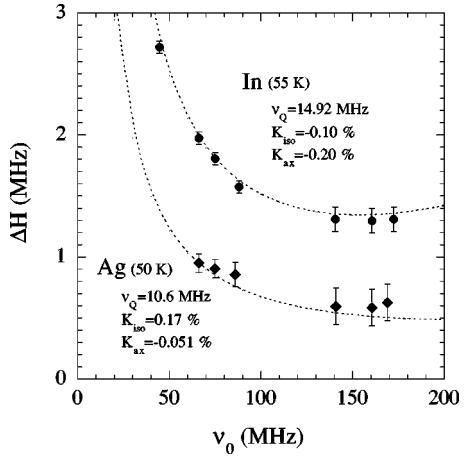

FIG. 5. Dependence on applied magnetic field $H_{\rm appl}$ of central NMR line splitting of ^{63}Cu NMR for 16e site in $YbXCu_4$ ($X=$Ag and In). Solid curves are splittings of the central NMR line calculated through the procedure described in the text.

of 75 MHz. The spectra for all the compounds have the general electric-quadrupole powder-pattern:[30] a second-order split central line and equally split satellite lines with maximum at $\theta=\pi/2$. The quadrupole-split spectra are assigned to ^{63,65}Cu on the 16e site with noncubic local symmetry. A nonzero asymmetry factor η of the electric field gradient (EFG) q at Cu nuclei is to result in shoulders on both sides of the central line and also at $\phi=\pi/2$ ($\theta=\pi/2$) of satellite lines.[31] Here θ is the angle of the applied field $H_{\rm appl}$ with respect to the principal Z axis of q, and ϕ the azimuthal angle. Lack of clear shoulders either on the central line or satellite lines indicates that the value of η in $YbXCu_4$ is rather small. The interval between the satellite lines, which was independent of $H_{\rm appl}$, gives a measure of quadrupole frequency ν_Q, and the value agrees with that obtained by the PQR measurements.

We have found that the splitting of central line varies with increasing $H_{\rm appl}$, as shown in Fig. 5 typically for $X=$Ag and In (data for In below 100 MHz are referred from Ref. 29). This is an indication that the splitting due to the second-order electric-quadrupole interaction is of the order of magnitude of axial Knight shift $K_{\rm ax}$, and the extent of the splitting is controlled by changing $H_{\rm appl}$: the anisotropic effects are proportional to $H_{\rm appl}$, whereas the second-order quadrupole splitting is proportional to $1/H_{\rm appl}$.

The quadrupole frequency ν_Q relates to q and the quadrupole moment Q of an observed nucleus as $\nu_Q=|3e^2qQ/2hI(2I-1)|$. q consists of contributions from the ionic charge on the lattice sites around an observed nucleus $q_{\rm lat}$ and the intra-atomic electron distribution $q_{\rm el}$ as[32]

$$q=(1-r_\infty)q_{\rm lat}+(1+R)q_{\rm el}, \tag{2.1}$$

where r_∞ and R are ionic Sternheimer antishielding factor and core correction factor, respectively. In the $YbXCu_4$ series, the valence of Cu ions on the 16e site is considered to be close to nonmagnetic Cu^{1+} with d^{10} electron configuration which gives rise to $q_{\rm el}\sim 0$. As was noted in Ref. 24 for $X=$In, the increase in $\nu_{\rm Q}$ originates from the increase in $q_{\rm lat}$ and, therefore, the decrease in the unit-cell volume.

Then we shall suppose that the magnetic shift tensor is also axially symmetric, and that the major axes of the electric field gradient and magnetic shift tensors are coincident. If this were not the present case, each of the quadrupole split lines would be split into four lines or severely broadened. For the case where axial Knight shift and second-order quadrupole effects are present simultaneously in the absence of quadrupole asymmetry ($\eta \sim 0$), following Jones *et al.*[33] and McCart,[34] the two maxima occur at $\cos\theta_{\mathrm{I}}=0$ and at

$$\cos\theta_{\mathrm{II}}=\pm\left\{\frac{5}{9}-\frac{8a\nu_0^2}{3\nu_Q^2[I(I+1)-3/4]}\right\}^{1/2}, \tag{2.2}$$

where $a=K_{\mathrm{ax}}/[1+K_{\mathrm{iso}}]$, and K_{iso} is isotropic Knight shift. The 5/9 term is that for the electric-quadrupole effect alone. For the NMR spectra obtained in the field sweeping procedure at a constant frequency ν_0, the resonance fields H_{I} and H_{II} at the two maxima of central line are given by the following equations:

$$h\nu_0(\theta_{\mathrm{I}})=\gamma_n\hbar H_{\mathrm{I}}(1+K_{\mathrm{iso}}-K_{\mathrm{ax}})+\frac{hb}{\nu_0}, \tag{2.3}$$

$$h\nu_0(\theta_{\mathrm{II}})=\gamma_n\hbar H_{\mathrm{II}}\left\{1+K_{\mathrm{iso}}+K_{\mathrm{ax}}\left(\frac{2}{3}-\frac{a\nu_0^2}{2b}\right)\right\} -h\left\{\frac{16b}{9\nu_0}-\frac{a^2\nu_0^3}{4b}\right\}. \tag{2.4}$$

Here, $b=(\nu_Q^2/16)[I(I+1)-3/4]$. These two equations can then be solved for K_{iso} and K_{ax} with the experimental values of H_{I} and H_{II} at the two maxima and ν_Q determined by PQR measurements. The results for ^{63}Cu on the 16*e* site in each of YbXCu$_4$ compounds are plotted in Fig. 6 against temperature. For $X=$Au, the central line exhibits a large CW-type broadening with decreasing temperature, which made the two maxima unclear at low temperatures. Then we calculated K_{iso} and K_{ax} only for the NMR spectra above $\sim$55 K. K_{ax} has a similar temperature dependence in shape to K_{iso} except for $X=$Cd.

The splitting of the central line is given by[33]

$$\Delta_{\mathrm{I,II}}=\frac{25b}{9\nu_0}-\frac{5a\nu_0}{3}+\frac{a^2\nu_0^3}{4b}, \tag{2.5}$$

and, as is drawn by dotted curves, the field dependence of the splitting shown in Fig. 5 can be reproduced satisfactorily with the values of K_{iso} and K_{ax} obtained above in spite of our crude approximations. In the analysis of the central NMR line in our previous paper for YbInCu$_4$,[29] we evaluated only K_{iso} assuming $K_{\mathrm{ax}}\sim 0$, and incorrectly conjectured the increase of splitting with H_{appl} to increase in ν_Q. In the present paper, however, we have found from interval between the satellite lines that ν_Q is independent of H_{appl}.

At high temperatures, a negative contribution to the isotropic Knight shift K_{iso} for the compounds with $X=$Au, Ag, In, and Cd exhibits a CW-type increase. At low temperatures, however, each of K_{iso} exhibits a distinct behavior: a monotonous large increase for $X=$Au, a step decrease at 45 K for $X=$In, and a broad maximum around 40 K for $X=$Ag and around 140 K for $X=$Cd. In contrast, K_{iso} for $X=$Mg has a large positive value which increases monotonously with decreasing temperature. K_{iso} for $X=$Tl is positive and relatively insensitive to the variation of temperature. The axial Knight shift K_{ax} of ^{63}Cu in each of YbXCu$_4$ except for $X=$Au and In has rather small values.

For the compounds with $X=$Cd and Tl at high temperatures, we found an additional small ^{63}Cu resonance line at a field between the two maxima of central line, as typically shown in Fig. 7 for YbCdCu$_4$. The additional single resonance line largely shifts with temperature, and is reasonably assigned to Cu on the 4*c* site with local cubic symmetry ($\nu_Q=0$). This provides evidence for the existence of X-Cu site disorder of about 10% or less that is estimated from the signal intensity. The ^{63}Cu Knight shift K for the 4*c* site, determine at peak intensity, is plotted in Fig. 8 against temperature. For $X=$Cd below $\sim$140 K, the resonance line for the 4*c* site approaches the H_{II} maximum of the central line for the 16*e* site, which makes it difficult to deduce a reliable value of K. At high temperatures, the negative K for the 4*c* site of the compounds with $X=$Cd and Tl exhibits a CW-type increase. K for $X=$Tl reaches a minimum around 50 K.

III. DISCUSSION

A clear indication of Yb^{3+} ions in YbXCu$_4$ at high temperatures is given by the Curie-Weiss-type magnetic susceptibility and Knight shift, which revealed independent excitations between CEF split energy levels of $4f^{13}$. In a cubic crystal field, $^2F_{7/2}$ Hund's rule ground state splits into two doublets (Γ_6 and Γ_7) and one quartet (Γ_8). Neutron scattering measurements[35] for YbAuCu$_4$ and YbAgCu$_4$ gave a CEF scheme with a Γ_7 ground state, a Γ_8 quartet excited state Δ_1 above the ground state, and a Γ_6 doublet state Δ_2 above Γ_8 level. The CEF splittings Δ_1 and Δ_2 have been estimated as 3.89 and 2.99 meV for YbAuCu$_4$, and 9.3 and 7.2 meV for YbAgCu$_4$. Characteristic behaviors of the magnetic susceptibility $\chi(T)$ data at low temperatures (Fig. 1) have been explained quantitatively with the energy level scheme.[1] We will base our discussion on the analysis of the isotropic Knight shift data.

A. K_{iso} versus χ plots

Knight shift $K(T)$ of ^{63}Cu in rare-earth compounds is generally related to the magnetic susceptibility $\chi(T)$ of the rare-earth ions with a transferred hyperfine field H_{hf} as

$$\vec{K}(T)=K_s+\frac{\mathbf{H}_{\mathrm{hf}}}{\mu_B N}\vec{\chi}(T), \tag{3.1}$$

where K_s is an on-site contribution which consists of a conduction electron term and a field-induced Van Vleck orbital term

$$K_s=K_c+K_{\mathrm{VV}}. \tag{3.2}$$

Here, we neglected contributions from the Landau and ion-core diamagnetic terms which are generally much smaller

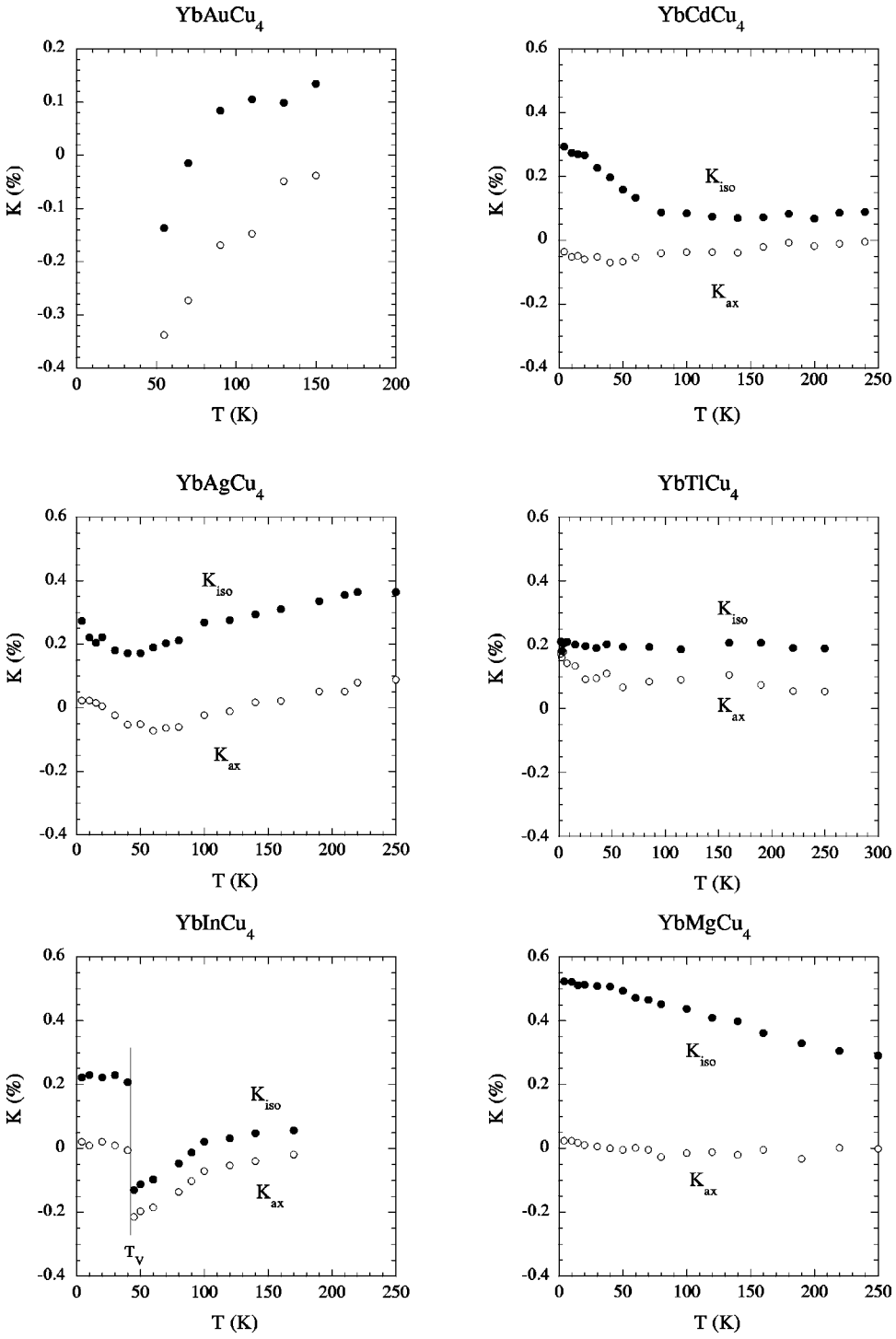

FIG. 6. Temperature dependence of isotropic and axial Knight shifts of ^{63}Cu on 16*e* site in each of YbXCu$_4$ compounds with X = Au, Ag, In, Cd, Mg, and Tl, calculated from resonance fields at two maxima of the central NMR line.

than those from the paramagnetic terms for transition-metal elements. Figure 9 shows $K_{\rm iso}$ versus χ plots for ^{63}Cu on the 16*e* site in each of the YbXCu$_4$ compounds with temperature being the implicit parameter. The plots for X = Au, Ag, and In (HT phase) are on corresponding straight lines drawn in the figure, and the slope gives $H_{\rm hf}=-0.63$, -0.72, and -0.45 kOe/μ_B, respectively, which originate from transferred hyperfine couplings with the $4f$ spin of the neighboring Yb ions. The intersection of the straight line and vertical $K_{\rm iso}$ axis gives an estimate of the temperature-independent term K_s at high temperatures as 0.33, 0.46, and 0.17 % for X = Au, Ag, and In, respectively. For X = In, the value of K_s in the HT phase is smaller than 0.23% in the LT phase.

In contrast, $K_{\rm iso}$ versus χ plots for the compounds with X = Cd and Tl exhibit somewhat complicated behavior. For X = Cd, the plots above 140 K are roughly on a straight line which gives $H_{\rm hf}=-0.52$ kOe/μ_B and $K_s=0.15\%$. Below 140 K, $K_{\rm iso}$ exhibits a large increase in spite of the fact that the χ data tend to saturate. If we reasonably assume that the on-site Knight shift K_c is near independent of temperature, the plots indicate that the negative $H_{\rm hf}$ begins to decrease below 140 K, changes sign at around 50 K, and increases to

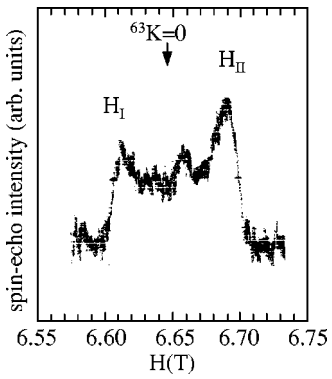

FIG. 7. An additional ^{63}Cu resonance line originated from Cu on the 4*c* site of $YbCdCu_4$ at 75 MHz and 260 K, observed at a field between two maxima of central NMR line.

0.47 kOe/μ_B at 4.2 K. For $X=$Mg, we did not observe the linear relation between $K_{\rm iso}$ and χ within our experimental range. The value of K_s can be estimated as about 0.10% by fitting the $K_{\rm iso}$ data above 150 K with a CW-type law $K=K_s+\alpha/(T+\theta)$ with $\theta=72$ K deduced from the χ data. Then the $K_{\rm iso}$ versus χ plots for $X=$Mg indicates that $H_{\rm hf}\sim 2.7$ kOe/μ_B at 250 K and increases to ~ 5.4 kOe/μ_B at 30 K. For $X=$Tl, the near temperature independent behavior of $K_{\rm iso}$ gives K_s of about 0.20%.

Figure 10 shows K versus χ plots for ^{63}Cu on the 4*c* site in the compounds with $X=$Cd and Tl. The plots for $X=$Cd above 140 K are on a straight lines, which is consistent with the $K_{\rm iso}$ versus χ plots for the 16*e* site. The plots for the 4*c* site gives $H_{\rm hf}=-3.22$ kOe/μ_B and $K_s=0.17\%$. The value of K_s at the 4*c* site is in good agreement with that at the 16*e* site. The plots for $X=$Tl are somewhat scattered because of the small χ values.

B. Variation of physical quantities with the species of *X* atoms

In this subsection, we explore the extent to which the various physical properties and their variations with the species of *X* atoms can be described by the unit-cell volume, *sf* mixing, and density of states of *sf* resonance bands at the Fermi level.

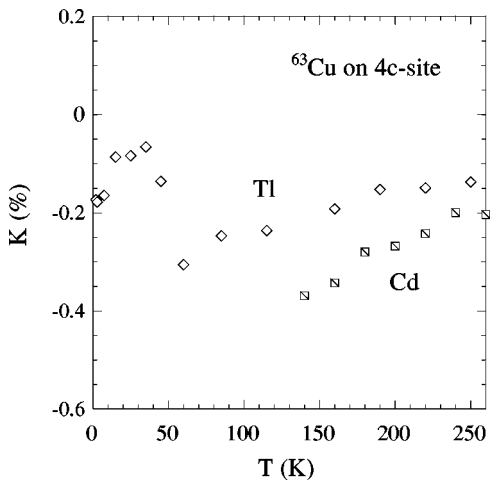

FIG. 8. ^{63}Cu Knight shift of ^{63}Cu on the 4*c* site in $YbXCu_4$ with $X=$Cd and Tl as a function of temperature.

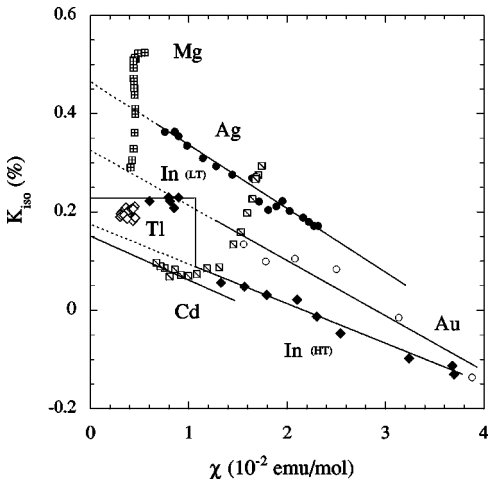

FIG. 9. Isotropic Knight shift versus magnetic susceptibility plots for ^{63}Cu on the 16*e* site of $YbXCu_4$ ($X=$Au, Ag, In, Cd, Tl, and Mg) with temperature being the implicit parameter.

For the compounds with $X=$Au, Ag, and In, as is shown in Fig. 11, we have found rather good correlation between the on-site Knight shift K_s (closed circles) and the coefficient of low-temperature electronic specific heat γ (open circles). γ is proportional to the density of states $N(E_F)$ of the *sf* conduction bands. Then we may conclude that K_s is a measure of $N(E_F)$ around the 16*e* site, and the orbital term $K_{\rm VV}$ in Eq. (3.2) is considered to be very small, consistent with the d^{10} electron configuration of Cu ions. The compounds can be classified into three groups: $X=$Ag and In; $X=$Cd, Tl, and Mg; and $X=$Au.

Mixed-valence regime close to heavy-Fermion state. For $YbAgCu_4$, we have found that the lattice constant *a* takes a minimum at around 40 K, as for $YbInCu_4$.[24] Figure 12 shows the dependence of isotropic Knight shift $K_{\rm iso}$ on the unit-cell volume v_c with temperature being the implicit parameter for

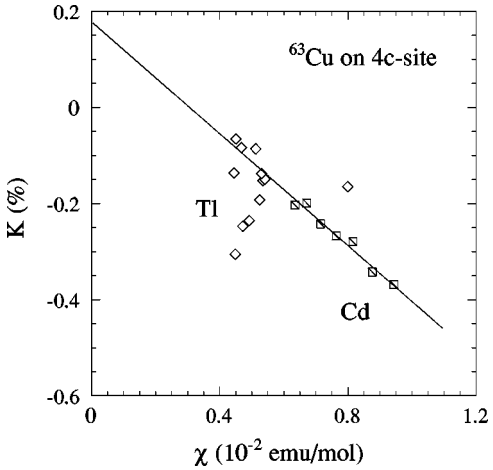

FIG. 10. Knight shift versus magnetic susceptibility plots for ^{63}Cu on the 4*c* site of $YbXCu_4$ ($X=$Cd and Tl) with temperature being the implicit parameter.

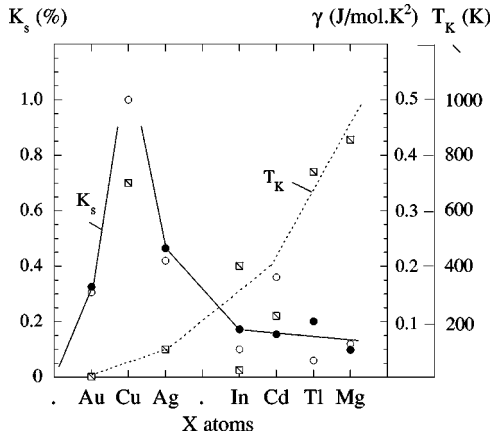

FIG. 11. Schematic phase diagram for YbXCu$_4$ series. Variations with the species of X atoms of on-site Knight shift K_s (closed circles), and electronic specific heat coefficient (open circles) and Kondo temperature (open squares) cited from Refs. [1–3,10,14–21].

each of the compounds with $X=$Ag and In. Below 100 K, $K_{\rm iso}$ for $X=$Ag decreases linearly with decreasing v_c with a slope $dK_{\rm iso}/d[v/v(300)]=0.675$. Here, the decrease in $K_{\rm iso}$ corresponds to the increase in χ. In the HT phase of YbInCu$_4$, the $K_{\rm iso}$ versus v_c plots between T_V and 140 K are also on a straight line with a slope of $dK_{\rm iso}/d[v/v(300)]=1.16$. The linear relation between $K_{\rm iso}$ and v_c indicates that the magnetism of the compounds at low temperatures is controlled by the unit-cell volume. As the unit-cell volume expansion is favorable for nonmagnetic Yb^{2+} rather than magnetic Yb^{3+} ions, we may conclude that YbAgCu$_4$ exhibits a crossover around 40 K from the localized moment state to a mixed-valence state. Sufficient sf mixing[3,20,24–26] appears to allow the mixed-valence state. The values of both K_s and γ for $X=$Ag are larger than those for $X=$In indicating that YbAgCu$_4$ is located close to the heavy-Fermion state.

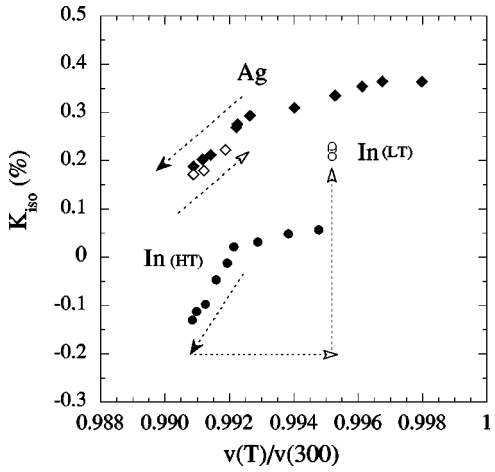

FIG. 12. Dependence of isotropic Knight shift on the unit-cell volume with temperature being the implicit parameter for the compounds with $X=$Ag and In. Open diamonds for $X=$Ag are the data below 40 K, and open circles for $X=$In are the data below 45 K. Arrows are in a direction to lowering temperature.

As can be seen in Fig. 12, the values of $K_{\rm iso}$ for YbAgCu$_4$ below 40 K (open diamonds) are somewhat smaller in magnitude than the values expected for the same unit-cell volume above 40 K (closed diamonds). For YbInCu$_4$ below the first-order valence transition at 45 K, the negative contribution to $K_{\rm iso}$ exhibits a step decrease with the volume expansion of about 0.5%. The extent of the $K_{\rm iso}$ step for the volume expansion is, however, about 75% of an expected value obtained by the extrapolation of the best fit line for the data below 140 K. These results indicates that the nonmagnetic behavior at low temperatures of both YbAgCu$_4$ and YbInCu$_4$ cannot be described only by the Kondo volume expansion model.[36]

Mixed-valence regime far from heavy-Fermion state. The small values of K_s for the compounds with $X=$Cd, Mg, and Tl suggest that $N(E_F)$ of the sf conduction bands are comparable in magnitude with that for YbInCu$_4$. The rather high T_K and existence of local maximum in χ around 260 K for $X=$Tl and 130 K for $X=$Mg (Fig. 2) indicate that these compounds are in a mixed-valence state somewhat far from the heavy-Fermion state.

In the present NMR data, the compounds with $X=$Cd and Mg are characterized by strongly temperature-dependent transferred hyperfine couplings $H_{\rm hf}$. Similar variations in $H_{\rm hf}$ with temperature have been observed in heavy-Fermion compounds of $CeAl_3$, $CeCuSb_2$, $CeAl_2$, and so on,[37–39] in which it was attributed to CEF interactions.[39] If the hyperfine field is anisotropic, the restricted symmetry of the Γ_7 ground state wave function will cause it to couple differently to neighboring Cu nuclei than the Γ_8 excited state wave function. Then $H_{\rm hf}$ is expected to decrease at low temperatures, removing the degeneracy of CEF splittings. Very large variations in $H_{\rm hf}$ observed for the YbXCu$_4$ compounds with $X=$Cd and Mg, however, cannot be explained only by removing the degeneracy of CEF splittings with lowering temperature.

It is worth noting that $H_{\rm hf}$ takes a constant value at high temperatures where χ data follow a Curie-Weiss law. $H_{\rm hf}$ markedly increases coincident with the saturated behavior of χ for $X=$Cd below $\simeq 140$ K, and with the decrease in χ for $X=$Mg below ~ 300 K. The variation in the CEF energy level scheme of Yb ions, when the system transforms into the mixed-valence state, is expected to largely change the anisotropic mixing between the Yb $4f$ hole states and conduction electrons and, therfore, the trasferred hyperfine coupling tensor. As can be seen in Fig. 6 the Knight shift of ^{63}Cu in the compound expected to be in the mixed-valence regime [compounds with $X=$Cd, Mg, Ag ($T<20$ K), In (LT phase)] is much more isotropic ($K_{\rm ax}\sim 0$) than in the localized spin regime.

Although the χ data for $X=$Cd shown in Fig. 2 has a temperature dependence which resembles that of heavy-fermion compounds, the large variation in $H_{\rm hf}$ with temperature and rather small value of K_s suggests that YbCdCu$_4$ also belongs to a group of mixed-valence compounds. For YbTlCu$_4$, the small values of both χ and $H_{\rm hf}$ do not allow any reliable analysis. A quantitative discussion on the variation of transferred interactions with CEF interactions in YbXCu$_4$ series will be presented elsewhere.

Localized moment regime. The very large CW-type behaviors of both K_{iso} and χ for $X=$Au can reasonably be ascribed to nearly localized moments of Yb^{3+}. In addition, rather large values of both K_s and γ indicate that $YbAuCu_4$ is in a heavy-fermion state. The contrasting behavior of $YbAuCu_4$ to $YbAgCu_4$, which have isoelectronic states, can be reasonably understood from the smaller lattice constant for $X=$Au than that for $X=$Ag,[1] which is favorable for the magnetic Yb^{3+} ions.

Schematic phase diagram. Finally, we propose a phase diagram for $YbXCu_4$ series illustrated in Fig. 11, which corresponds to Doniach's phase diagram.[40] In the figure, the on-site Knight shifts K_s at high temperatures are deduced from the $K_{iso}(T)$ data of ^{63}Cu on the 16*e* site, and γ and T_K are cited from various experiments. [1–3,10,14–21,41] The variation of K_s with the species of X atoms roughly correlates with that of γ except for $X=$Cd. The anomalously large γ for $X=$Cd is considered to consist not only of the conduction bands contribution but of a magnetic contribution. The phase diagram implies that the quantum critical point is located around the $YbCuCu_4$ compound.

IV. CONCLUSION

We have carried out a systematic ^{63}Cu NMR study on a set of isostructural ytterbium-based Kondo compounds $YbXCu_4$ with $X=$Au, Ag, In, Cd, Tl, and Mg. We have succeeded to deduce values of both isotropic and axial Knight shifts from the splitting of the central resonance of the electric quadrupole split NMR spectrum, taking a quadrupole frequency obtained by PQR measurements. The obtained values for K_{iso} and K_{ax} were able to reproduce satisfactorily the applied magnetic field dependence of the splitting between the two maxima of the central resonance.

K_{iso} versus χ plots for each of the compounds with $X=$Au, Ag, and In are on corresponding straight lines. For $YbAgCu_4$, we have found a local minimum around 40 K for both K_{iso} and the lattice constant. The linear dependence of K_{iso} on the unit-cell volume observed for 4.2–100 K though the K_{iso} minimum, similar to that observed below $\sim$140 K of $YbInCu_4$, indicates that the near nonmagnetic behavior of $YbAgCu_4$ below 40 K can mostly be explained by the small volume expansion.

In contrast, K_{iso} versus χ plots for $YbCdCu_4$ and $YbMgCu_4$ exhibit somewhat complex behavior: hyperfine field H_{hf} markedly increases associated with the saturated behavior of χ for $X=$Cd below $\simeq$140 K, and with the decrease in χ for $X=$Mg below $\sim$260 K. H_{hf} originates mainly from transferred hyperfine coupling between Cu nucleus and Yb $4f$ moment, and the large increase in H_{hf} is attributed to a variation of crystal-electric-field interactions as the system transforms into a mixed-valence state.

The variation with the species of X atoms of temperature-independent on-site contribution K_s to the Knight shift is found to correlate with that of the electronic specific heat coefficient γ (except for $X=$Cd), each of which give a measure of the density of states of conduction sf resonance bands. Then, using the values of K_s, γ, and T_K, we have proposed a phase diagram for $YbXCu_4$ series, which corresponds to the Doniach's phase diagram. $YbAuCu_4$ is classified to a localized regime, $YbAgCu_4$ and $YbInCu_4$ to a mixed-valence regime close to heavy Fermion state, and $YbCdCu_4$, $YbTlCu_4$, and $YbMgCu_4$ to a mixed-valence regime far from the heavy-fermion state.

ACKNOWLEDGMENTS

The authors wish to express their thanks to Professor M. Ishikawa, Institute for Solid State Physics, University of Tokyo, for his kindness in measuring the x-ray diffraction pattern of $YbAgCu_4$ at low temperatures. We are also grateful to Professor H. Shiba, Faculty of Science, Kobe University, for valuable discussions. Work at Los Alamos was performed under the auspices of the U. S. Department of Energy.

[1] J. L. Sarrao, C. D. Immer, Z. Fisk, C. H. Booth, E. Figueroa, J. M. Lawrence, R. Modler, A. L. Cornelius, M. F. Hundley, G. H. Kwei, J. D. Thompson, and F. Bridges, Phys. Rev. B **59**, 6855 (1999), and references therein.

[2] C. Rossel, K. N. Yang, M. B. Maple, Z. Fisk, E. Zirngiebl, and J. D. Thompson, Phys. Rev. B **35**, 1914 (1987).

[3] A. Severing, A. P. Murani, J. D. Thompson, Z. Fisk, and C.-K. Loong, Phys. Rev. B **41**, 1739 (1990).

[4] E. Bauer, E. Gratz, R. Hauser, Le Tuan, A. Galatanu, A. Kottar, H. Michor, W. Perthold, G. Hilscher, T. Kagayama, F. Oomi, N. Ichimiya, and S. Endo, Phys. Rev. B **50**, 9300 (1994).

[5] E. Bauer, P. Fischer, F. Marabelli, M. Ellerby, K. A. McEwen, B. Roessli, and M. T. Fernandes-Dias, Physica B **234-236**, 676 (1997).

[6] I. Felner and I. Nowik, Phys. Rev. B **33**, 617 (1986); I. Felner, I. Nowik, D. Vaknin, U. Potzel, J. Moser, G. M. Kalvius, G. Wortmann, G. Schmiester, N. Pillmayr, K. G. Prasad, H. de Waard, and H. Pinto, *ibid.* **35**, 6956 (1987); I. Nowik, I. Felner, D. Voiron, J. Beille, A. Najib, E. du Tremolet de Lacheisserie, and E. Gratz, *ibid.* **37**, 5633 (1988).

[7] B. Kindler, D. Finsterbusch, R. Graf, F. Ritter, W. Assmus, and B. Luthi, Phys. Rev. B **50**, 704 (1994).

[8] J. M. de Teresa, Z. Arnold, A. del Moral, M. R. Ibarra, J. Kamard, D. T. Adroja, and B. Rainford, Solid State Commun. **99**, 911 (1996).

[9] J. M. Lawrence, G. H. Kwei, J. L. Sarrao, Z. Fisk, D. Mandrus, and J. D. Thompson, Phys. Rev. B **54**, 6011 (1996).

[10] J. L. Sarrao, C. D. Immer, C. L. Benton, Z. Fisk, J. M. Lawrence, D. Mandrus, and J. D. Thompson, Phys. Rev. B **54**, 12 207 (1996).

[11] J. L. Sarrao, C. L. Benton, Z. Fisk, J. M. Lawrence, D. Mandrus, and J. D. Thompson, Physica B **223-224**, 366 (1996).

[12] J. M. Lawrence, S. M. Shapiro, and Z. Fisk, Phys. Rev. B **55**, 14 467 (1997).

[13] C. D. Immer, J. L. Sarrao, Z. Fisk, A. Lacerda, C. Mielke, and J. D. Thompson, Phys. Rev. B **56**, 71 (1997).

[14] A. L. Cornelius, J. M. Lawrence, J. L. Sarrao, Z. Fisk, M. F. Hundley, G. H. Kwei, J. D. Thompson, C. H. Booth, and F. Bridges, Phys. Rev. B **56**, 7993 (1997).
[15] M. J. Besnus, P. Hean, N. Hamdaoui, A. Herr, and A. Nayer, Physica B **163**, 571 (1990).
[16] P. Bonville, B. Canaud, J. Hammann, A. J. Hodges, P. Imbert, G. Jehanno, A. Severing, and Z. Fisk, J. Phys. I **2**, 459 (1992).
[17] P. Schlottmann, J. Appl. Phys. **73**, 5412 (1993).
[18] P. Weibel, M. Grioni, D. Malterre, B. Dardel, Y. Baer, and M. J. Besnus, Z. Phys. B: Condens. Matter **91**, 337 (1993).
[19] E. Bauer, R. Hauser, E. Gratz, K. Payer, G. Oomi, and T. Kagayama, Phys. Rev. B **48**, 15 873 (1993).
[20] J. M. Lawrence, G. H. Kwei, P. C. Canfield, J. G. DeWitt, and A. C. Lawson, Phys. Rev. B **49**, 1627 (1994).
[21] T. Graf, J. M. Lawrence, M. F. Hundley, J. D. Thompson, A. Lacerda, E. Haanappel, M. S. Torikachhvili, Z. Fisk, and P. C. Canfield, Phys. Rev. B **51**, 15 053 (1995).
[22] V. T. Rajan, Phys. Rev. Lett. **51**, 308 (1983).
[23] B. Coqblin and J. R. Schrieffer, Phys. Rev. **185**, 847 (1969).
[24] H. Nakamura, K. Nakajima, Y. Kitaoka, K. Asayama, K. Yoshimura, and T. Nitta, J. Phys. Soc. Jpn. **59**, 28 (1990); J. Magn. Magn. Mater. **90-91**, 1581 (1990); Physica B **171**, 238 (1990); H. Nakamura *et al.*, *ibid.* **206-207**, 364 (1995); J. Phys. Soc. Jpn. **65**, 168 (1996).
[25] P. G. Pagliuso, C. Rettori, S. B. Oseroff, J. Sarrao, Z. Fisk, A. Cornelius, and M. F. Hundley, Phys. Rev. B **56**, 8933 (1997).
[26] P. Weibel, M. Grioni, D. Malterre, B. Darbel, Y. Baer, and M. J. Besnus, Z. Phys. B: Condens. Matter **91**, 337 (1993); J. J. Joyce, A. B. Andrews, A. J. Arko, R. J. Barlett, R. I. R. Blythe, C. G. Olson, P. J. Benning, P. C. Canfield, and D. M. Poirier, Phys. Rev. B **54**, 17 515 (1996).
[27] K. Hiraoka, K. Kojima, T. Hihara, and T. Shinohara, J. Magn. Magn. Mater. **104-144**, 1243 (1995).
[28] K. Hiraoka, K. Murakami, S. Tomiyoshi, T. Hihara, and K. Kojima, Physica B **281-282**, 173 (2000).
[29] T. Koyama, M. Matsumoto, S. Wada, and J. L. Sarrao, Phys. Rev. B **63**, 172410 (2001).
[30] G. C. Carter, L. H. Bennett, and D. J. Kahan, *Metallic Shifts in NMR I* (Pergamon Press, Oxford, 1977).
[31] G. H. Stauss, J. Chem. Phys. **40**, 1988 (1964).
[32] M. H. Cohen and F. Reif, *Solid State Physics*, edited by F. Seitz and D. T. Turnbull (Academic, New York, 1957), Vol. 5.
[33] W. H. Jones, Jr., T. P. Graham, and R. G. Barnes, Phys. Rev. **132**, 1898 (1963).
[34] B. R. McCart, Ph.D. thesis, Iowa State University, Ames, Iowa, 1965.
[35] A. Severing, A. P. Murani, J. D. Thompson, Z. Fisk, and C.-K. Loong, Phys. Rev. B **41**, 1739 (1990).
[36] J. L. Sarrao, A. P. Ramirez, T. W. Darling, F. Freibert, A. Migliori, C. D. Immer, Z. Fisk, and Y. Uwatoko, Phys. Rev. B **58**, 409 (1998).
[37] M. J. Lysak and D. E. MacLaughlin, Phys. Rev. B **31**, 6963 (1985).
[38] T. Koyama, M. Matsumoto, S. Wada, Y. Muro, and M. Ishikawa (unpublished).
[39] D. E. MacLaughlin, O. Pena, and M. Lysak, Phys. Rev. B **23**, 1039 (1981).
[40] S. Doniach, Physica B **91**, 231 (1977).
[41] Z. Fisk, J. D. Thompson, and H. R. Ott, J. Magn. Magn. Mater. **76-77**, 637 (1988).